Liquid Crystals
Publication details, including instructions for authors and subscription information:
http://www.informaworld.com/smpp/title~content=t713926090

Electroclinic effect around a smectic A-chiral nematic phase transition

C. L. Folcia; J. Ortega; J. Etxebarria

Online publication date: 11 November 2010

To cite this Article Folcia, C. L. , Ortega, J. and Etxebarria, J.(2002) 'Electroclinic effect around a smectic A-chiral nematic phase transition', Liquid Crystals, 29: 6, 765 — 773
To link to this Article: DOI: 10.1080/02678290210130847
URL: http://dx.doi.org/10.1080/02678290210130847

LIQUID CRYSTALS, 2002, VOL. 29, NO. 6, 765–773

Taylor & Francis
Taylor & Francis Group

Electroclinic effect around a smectic A–chiral nematic phase transition

C. L. FOLCIA, J. ORTEGA*, and J. ETXEBARRIA
Departamento de Física de la Materia Condensada,
*Departamento de Física Aplicada II, Facultad de Ciencias,
Universidad del País Vasco, Apartado 644, 48080 Bilbao, Spain

(*Received 3 November 2001; accepted 14 January 2002*)

We present measurements of the dynamics of the electroclinic effect around a smectic A–chiral nematic transition. The phenomenon has been studied between 1 kHz and 1 MHz, extending by one order of magnitude the frequency range of previous studies. The results have unambiguously allowed us to distinguish two additive mechanisms in the generation of the optical tilt. A model to explain the physical origin of both mechanisms is presented. The first mechanism (fast) is the only bulk process intrinsic to the material and behaves normally at the transition, in the sense that both the magnitude of the tilt as well as the relaxation time have the expected temperature dependence. On the other hand, the second mechanism (slow) is not properly an electroclinic effect, but a surface-mediated effect driven by elastic forces. This explains the apparent anomalous behaviour of the phenomenon reported in the literature one decade ago.

1. Introduction

The electroclinic effect (EE) in chiral nematics was discovered in 1989 by Li *et al* [1]. The phenomenon involves the appearance of an optical tilt induced by an electric field perpendicular to the molecular director, in a similar way to the conventional EE in orthogonal smectics composed of chiral molecules. To observe the effect it is necessary to have a chiral nematic (N*) material in the planar geometry with the helix unwound by the effect of the cell surfaces. In addition, the material should display a negative dielectric anisotropy in order to avoid a Fréedericksz transition.

Given these requirements and the small magnitude of the induced tilt θ, there have not been many studies published on this effect and, actually, even the nature of the phenomenon is not well understood. The size of θ is larger at temperatures close to a phase transition to a smectic phase. At a SmA–N* transition, θ drops suddenly to a small fraction of the value just below the transition. This temperature behaviour is interesting because, in principle, available theories predict a much slower tilt variation [2, 3]. On the other hand, the dynamical behaviour of the EE is also unexpected near the SmA–N* transition [4–6]. On heating the material from the SmA phase, the electroclinic relaxation time τ grows abnormally near the transition, despite the fact that θ decreases monotonically in this temperature region. Well inside the N* phase the EE is very small and extremely fast ($\tau < 1\,\mu s$).

In this work we present measurements of the dynamics of the EE around a SmA–N* transition. The phenomenon has been studied up to a frequency $\nu = 1$ MHz, extending by one order of magnitude the frequency range of previous works. The results are considerably clearer than those from previous studies and have unambiguously allowed us to distinguish two physical mechanisms in the generation of the optical tilt. We propose a model which takes account of the physical origin of both mechanisms. One of the mechanisms (fast) is intrinsic to the material and the other (slow) is induced by an effect at the sample surfaces. The fast mechanism does not behave abnormally at the SmA–N* transition, in the sense that both the tilt magnitude as well as the relaxation time associated with this mechanism follow, at least qualitatively, the expected trends.

2. Experimental

The material studied was a commercial mixture, SCE9 (Merck), with the following phase sequence SmC*–61°C–SmA–91.7°C–N*–120°C–I. Here I and SmC* refer to the isotropic and chiral smectic C phases, respectively. The material is suitable for measuring the EE in the N* phase since it shows pitch compensation for samples with thickness $d < 30\,\mu m$ and has a negative dielectric

*Author for correspondence; e-mail: wmpetecj@lg.ehu.es

Liquid Crystals ISSN 0267-8292 print/ISSN 1366-5855 online © 2002 Taylor & Francis Ltd
http://www.tandf.co.uk/journals
DOI: 10.1080/02678290210130847

anisotropy. The relaxational behaviour of the EE in this material has been studied up to 100 kHz in previous work [6].

The experiment was performed using a commercial planar cell (E.H.C., Japan) with thickness $d = 2.8\,\mu m$ and area $4 \times 4\,mm^2$. The electric field was applied through semi-transparent high conductivity ITO electrodes ($\sim 10\,\Omega$/square). Sine wave voltages in the range 1–10 V (peak values) were used for the measurements. The temperature stability was 0.1°C. The light source was a stabilized He-Ne laser with wavelength $\lambda = 0.6328\,\mu m$. The sample was placed between crossed polarizers with an angle of 22.5° between the director axis and the first polarizer. The transmitted light was detected with a photomultiplier. The d.c. component of the signal (I_0) was measured with a voltmeter and the a.c. component (I) with a high frequency lock-in amplifier. The tilt angle is simply $\theta = I/4I_0$. This experimental set-up is highly accurate, since the imperfections of the optical components do not introduce significant errors in the measured tilts. In fact, if the polarizers are not perfect, but have parasitic ellipticities p and q, and a possible misetting of the crossed polarizer position δY is considered, the resulting measured angle is

$$I/4I_0 = \theta[1 + 2\delta Y - \sqrt{2}(p - q)\cot(\Delta/2)]$$

where Δ is the sample retardation and θ the true tilt. Typical values of $\delta Y \approx 0.25°$ and $|p - q|$ of the order of 10^{-2}–10^{-3} can be considered in our case. With these values an error in θ lower than 1% is expected.

The frequency response of the EE was examined between 1 kHz and 1 MHz. Below 1 kHz electrohydrodynamic instabilities begin to appear for voltages $V \sim 10$ V, and grow substantially as the frequency is diminished.

3. Experimental results

In a first step of our study we performed measurements of the induced tilt θ as a function of the driving voltage V for different temperatures for the SmA and N* phases. The result for 10 kHz is represented in figure 1. The response is clearly linear for all the temperatures. This is in contrast to the non-linear θ vs. V dependence reported in [3], which was explained as being due to heating of the (conductive) sample as a consequence of the Joule effect. The linear (θ, V) relationship was also checked at higher frequencies.

Next the amplitude and phase of the signal were determined as a function of the frequency for a set of temperatures. All the measurements in the present study were performed with a driving voltage of 1 V. It was found that the amplitude data provide mainly information about the magnitude of the tilt, whereas the phase is more sensitive to the dynamical aspects of the EE.

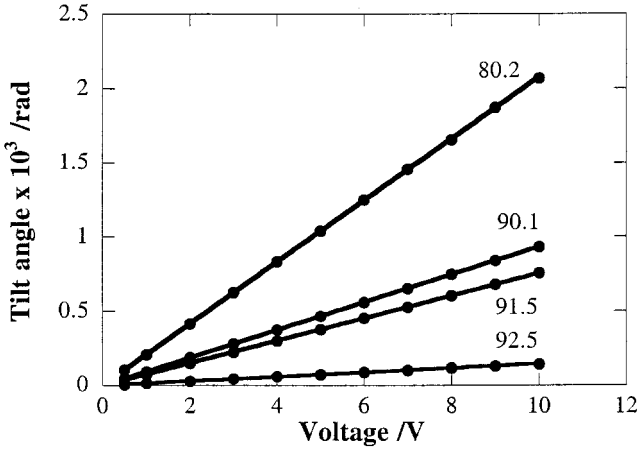

Figure 1. Tilt angle versus applied voltage in three representative temperature regions: at low temperatures far from the transition (80.2°C), for the SmA phase close to the transition point (90.1 and 91.5°C), and inside the N* range (92.5°C). The fits correspond to straight lines passing through the origin. The measurements were performed at low frequency (10 kHz).

Initially the results were analysed assuming a simple Debye relaxation process. In these conditions, the time dependence of the induced tilt $\Theta(t)$ is given by the expression

$$\Theta(t) = \frac{\mu}{a}\frac{E_0 \exp(i2\pi\nu t)}{1 + i\nu\tau} \tag{1}$$

where μ is the electroclinic coupling constant between the tilt and the electric field and a is proportional to $(T - T_0)$, where T is the temperature and T_0 is the SmC*–SmA transition temperature. The driving field is represented by $E = E_0 \exp(i2\pi\nu t)$, where ν is the frequency and τ is a characteristic relaxation time. The amplitude of the signal is

$$\Theta_0(\nu) = \frac{\mu E_0/a}{(1 + \nu^2\tau^2)^{1/2}} \tag{2}$$

and the phase shift

$$\delta = -\tan^{-1}(\nu\tau). \tag{3}$$

Figure 2 shows the tilt amplitude for $\nu = 0$, $\theta \equiv \theta_0(\nu = 0)$, versus temperature. These values were obtained from the extrapolation of the amplitudes to zero frequency according to expression (2). The results are similar to those reported earlier [6]. As the temperature decreases to the SmC* phase, the induced tilt shows the characteristic pretransitional divergence, as expected. On the other hand, at $T = 91.8$°C the tilt angle drops very abruptly

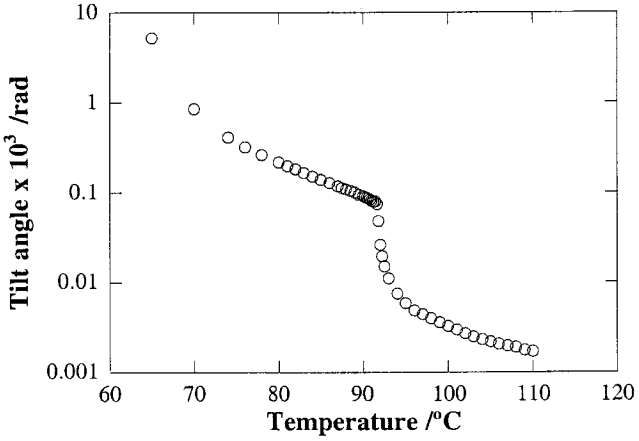

Figure 2. Induced optical tilt (logarithmic scale) versus temperature. The data are extrapolations of the tilt amplitude to null frequency. The driving voltage was 1 V and the sample thickness 2.8 μm.

to a value more than one order of magnitude smaller. Finally, in the N* phase θ goes smoothly to zero as the temperature increases.

As found in previous work [2, 3], the temperature dependence of θ above the SmA–N* transition is anomalous. The tilt variation is so strong that no reliable fit of the results can be obtained in the framework of available theories. In principle, θ should behave as the square of the smectic order parameter $|\Psi|^2$; this law rules out the existence of any cusp at the transition temperature and predicts a much slower variation of θ for any election of a realistic critical exponent α [2]. We will point out below the reason for this peculiar behaviour.

As previously mentioned, the dynamics of the EE were mainly investigated by means of measurements of the phase shift. To obtain δ it was necessary to deconvolute the sample response from the response time of the electronic circuitry. Here we include the RC time constant of the cell, the finite response time of the photomultiplier and the phase drift of the lock-in. All these effects produce a spurious phase delay δ_{elec}, which contributes to the total measured phase δ_T in the form

$$\delta_T = \delta_{elec} + \delta. \quad (4)$$

δ_{elec} was determined by measuring δ_T over the whole frequency range at two different temperatures in the SmA phase far away from the SmA–N* transition, where it is well known that the electroclinic relaxation follows a pure Debye process. Subtracting δ_T at both temperatures we get

$$\tan(\delta_T^{(1)} - \delta_T^{(2)}) = \tan(\delta^{(1)} - \delta^{(2)}) = -\frac{(\tau_1 - \tau_2)v}{1 + \tau_1\tau_2 v^2} \quad (5)$$

where the super-indices 1, 2 refer to both the temperatures and τ_1, τ_2 are the respective relaxation times. Provided that the selected temperatures exhibit very different relaxation times, an excellent fit to expression (5) can be performed, and results in a very accurate determination of τ_1 and τ_2. (In our experiment $\tau_1 = 44.7$ μs for $T_1 = 65$°C and $\tau_2 = 6.3$ μs for $T_2 = 70$°C). Once the relaxation times are known, δ_{elec} can be obtained straightforwardly using the expression

$$\delta_{elec} = \delta_T + \tan^{-1}(v\tau) \quad (6)$$

at either of the two temperatures. Following this procedure δ_{elec} was determined over the whole frequency range within an estimated error smaller than 1°.

Figure 3 shows typical profiles of $\tan\delta$ versus v around the SmA–N* transition. Below 90°C and above 92.5°C the points fit very well to a straight line, which means that the relaxation processes follow the Debye model. However, a clear deviation from linearity is observed between these temperatures. It is in this region where it is noted in previous reports that an unexpected slowing of the electroclinic response occurs in this [6] and other materials [4, 5]. In these papers a single apparent relaxation time τ_{eff} was determined due to the restricted frequency range of the measurements. However, the existence of at least two competing mechanisms was suspected, since τ_{eff} showed a slight dependence on v [5]. Our $\tan\delta$ data clearly confirm this hypothesis, the deviation from the Debye model being particularly evident in the range 90.6–92.0°C. In this region we have analysed the

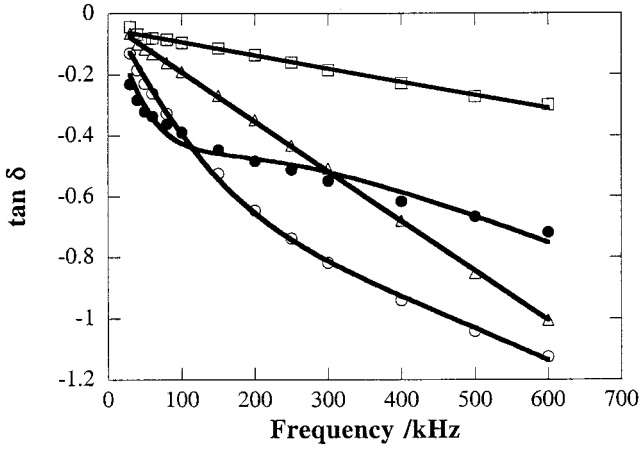

Figure 3. Tangent of the phase angle δ between the induced tilt and the applied field as a function of frequency at several temperatures in the anomalous region. Deviations from the Debye model are evident for 91.4°C (open circles) and 91.8°C (solid circles). Data at 90°C (triangles) and 92.5°C (squares) give almost straight lines. These temperatures mark approximately the limits of the anomalous region. Continuous lines are fits to equation (7).

results assuming two independent relaxation processes:

$$\Theta(t) = \frac{\mu}{a}\left(\frac{1}{1+\mathrm{i}v\tau_f} + \frac{x}{1+\mathrm{i}v\tau_s}\right)E_0 \exp(\mathrm{i}2\pi vt) \qquad (7)$$

where τ_f and τ_s are the relaxation times for the fast and slow processes, respectively, and x stands for the relative contribution to the induced tilt of the slow mechanism. The curves representing tan δ versus frequency near the phase transition were fitted to an expression deduced from equation (7). Acceptable fits were obtained in general (figure 3). The relaxation times τ_f and τ_s obtained, together with τ_{eff} are plotted as a function of temperature in figure 4. In this figure τ_{eff} was obtained from the slope of tan δ versus v for frequencies smaller than 100 kHz (τ_{eff} is represented for the whole range in figure 5).

Although the τ_s data scatter a lot, it can be said that, in general, τ_s is about one order of magnitude larger than τ_f. It is worth pointing out that when the slow mechanism is not really significant, the fitted values are not very precise. Probably, the coexistence of the two mechanisms is spread out over a wider temperature range, but when the proportion x of the slow mechanism becomes small and/or τ_s is of the order of τ_f the fitting process is ambiguous and unreliable. In this way, figure 4 must be considered to reflect general tendencies rather than to represent accurate determinations of τ_f and τ_s.

The relative contribution of the slow mechanism, x, is depicted in figure 6. This parameter is positive and reaches values higher than unity very close to the transition. This means that both electroclinic processes sum their contributions, and the slow mechanism is unexpectedly important (larger than the usual electroclinic process) at the transition point.

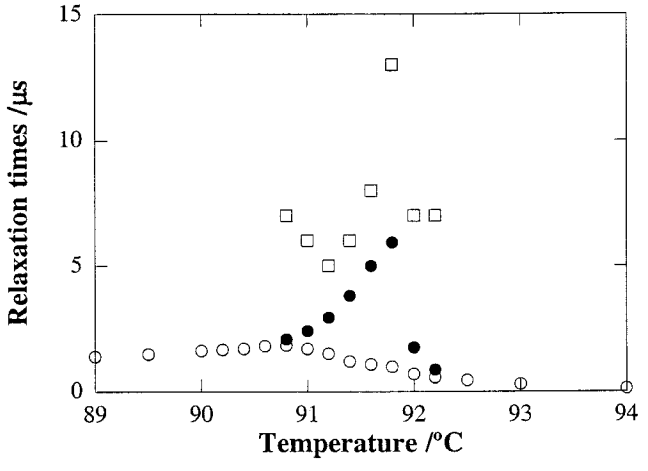

Figure 4. Temperature dependence of the fast relaxation process τ_f (open circles), slow relaxation process τ_s (squares) and τ_{eff} (solid circles). Below 90.5°C and above 92.5°C τ_f and τ_{eff} coincide.

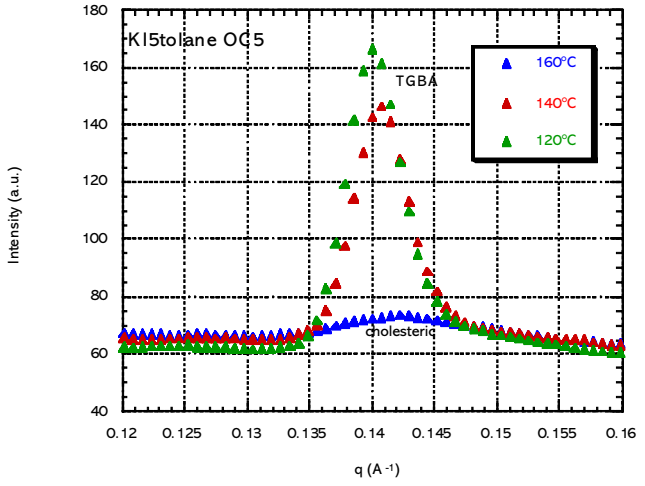

Figure 5. Response time of the EE as a function of temperature assuming only one effective mechanism. The data were deduced from the slope of the tan δ versus v curve for $v < 100$ kHz.

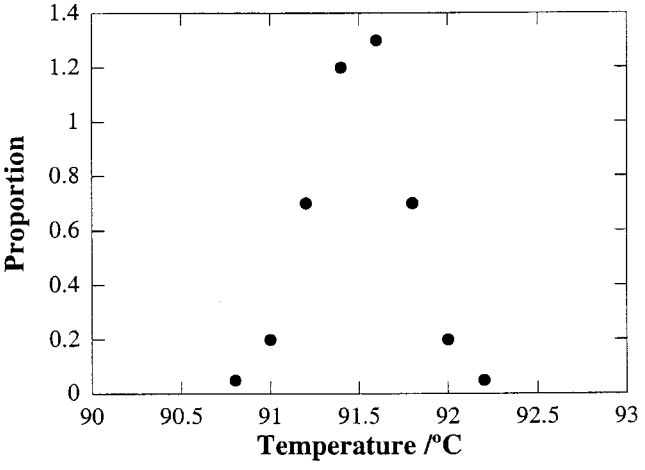

Figure 6. Temperature dependence of the proportion x of the electroclinic strength of the slow mechanism relative to the strength of the fast mechanism.

In figure 7 we have plotted the amplitude of the fast mechanism (solid circles) as deduced from the total tilt θ and the x value. We will argue below that this fast mechanism is the only contribution representing an intrinsic EE of the sample. As can be seen, its temperature dependence is much less abrupt near the transition than that of the θ points (open circles). Also, the cusp at the transition temperature has disappeared. Although our data do not allow us to perform an unambiguous fit in the critical region, it is evident that these points have qualitatively the temperature dependence expected by theory, i.e. can possibly behave as $|\Psi|^2$. Indeed, one

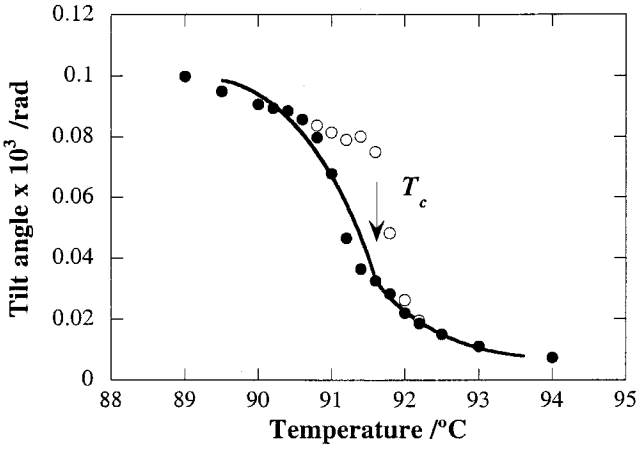

Figure 7. Amplitude of the fast mechanism (solid symbols) and total tilt (open symbols) around the SmA–N* transition. The continuous line is one possible fit to the renormalization-group prediction choosing a 3D-XY critical exponent $\alpha = -0.007$. The transition temperature T_c is marked with an arrow and corresponds to the inflection point of the curve for the black dots. This temperature coincides with the cusp of the total $\theta(T)$ curve.

possible fit to the renormalization-group expression:

$$\theta(T) = \pm A^{\pm} |T - T_c|^{1-\alpha}(1 \pm D_1^{\pm} |T - T_c|^{0.5}) + B(T - T_c) + \theta(T_c)$$

is presented in figure 7. Here T_c is the SmA–N* transition temperature, which is fixed by the position where the curve changes its curvature sign, $A^{\pm}$ and B are constants, the double sign referring to temperatures above and below the transition, respectively, and $D_1^{\pm}$ accounts for the so-called first order correction-to-scaling term. In figure 7 the critical exponent α was fixed to the prediction of the 3D-XY universality class, $\alpha = -0.007$, which is theoretically expected for a SmA–N transition involving broad SmA and N ranges [7]. Other fits giving different values of α are also possible, i.e. our measurements do not allow unequivocal determination of a particular universality class. However, as reported also in earlier work [2, 3], in no case can any acceptable fit be carried out with the complete $\theta(T)$ curve, due to its sharp behaviour at T_c. This apparent anomaly is then simply due to the fact that an important contribution to the tilt comes from a second process which is particularly important near the transition. We will discuss the nature of the two processes in the next section.

4. Discussion

From the temperature dependences of τ_s and x found previously, it seems reasonable to propose that the slow mechanism is closely related to the SmA–N* phase transition and should therefore be interpreted in terms of variables that change spontaneously at the transition. This point of view is different from that proposed by Li *et al.* [4, 5], who interpreted the increase of τ_{eff} on the SmA side of the SmA–N* transition as a consequence of an accidental proximity between the frequencies of the 'in-phase' and 'out-of-phase' amplitude fluctuations of the tilt and polarization, as described in [8]. In this approach it can be shown that the two mechanisms for the tilt dynamics must subtract their contributions in the SmA phase; $x < 0$ in equation (7). This is contrary to our results, which indicate unequivocally addition of both mechanisms ($x > 0$) both on the SmA and N* sides of the transition.

In a first approximation to the problem it can be considered that, following the fast orientation of the molecules by the electric field, a further contribution to the tilt can be originated by an increase in the smectic order. This is based on the assumption that the translational smectic order is almost essential for the EE, and the molecular interaction favouring the smectic layers is stronger when the molecules are equally oriented. Thus, the slow process can be supposed to be originated by an increase in $|\Psi|^2$ near the transition as a consequence of the field. In this scheme τ_s would be connected with the dynamics of the layers under the applied electric field. This idea is in accordance with Monte Carlo simulations of bent-rod mesogens [9], which indicate that a nematic phase can gain smectic order under the influence of strong electric fields.

In order to check the validity of the above hypothesis, we measured the birefringence in the temperature range 89–94°C. Equipment based on a photoelastic modulator was used. The spontaneous change in birefringence at the phase transition is proportional to $|\Psi|^2$, therefore the birefringence should be different when a bias electric field is applied to the sample. The result is shown in figure 8. It is clear that almost no variation is detected, and therefore the proposed model must be rejected.

Next, a different approach is presented. This is based on the fact that the tilt angle observed near the phase transition is small. Thus, it is very likely that the tilt at the surfaces is larger than in the bulk. This is what happens for example if we assume that $|\Psi|^2$ at the surfaces is larger than inside the sample. In any case, a tilt profile results when the field is applied, and the material becomes twisted.

If $|\Psi|^2 = 0$ in the bulk (pure N*), the orientation at the surface is transmitted to the whole sample thickness via the twist elastic constant K_2. As will be shown below, this process is extremely slow and difficult to detect. In the SmA case this elastic mechanism is also operative but extremely hard to observe. Here the coupling is different for two reasons:

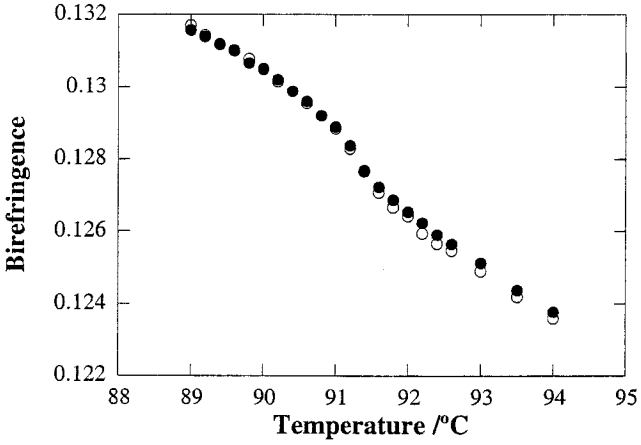

Figure 8. Temperature dependence of the birefringence without (closed symbols) and with a d.c. field of 4 V μm^{-1} (open symbols) around the SmA–N* transition.

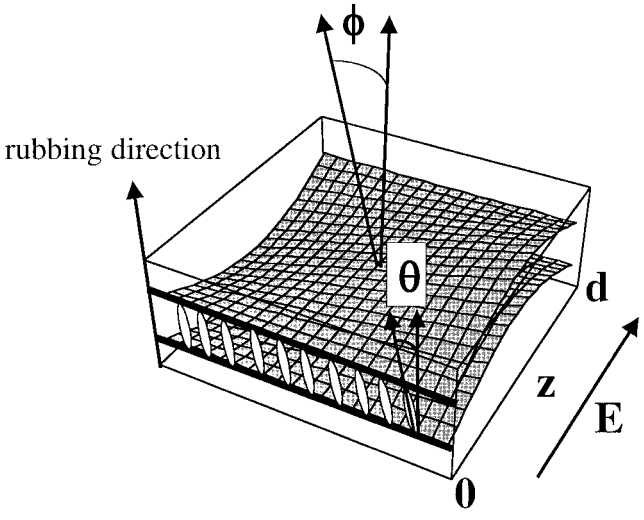

Figure 9. Profile of the layer orientation if twist distortions of the smectic layers as a whole are allowed. The rubbing direction is assumed to coincide with the layer normals at the cell surfaces. The molecular orientation is defined by two angles which depend on the coordinate z along the sample thickness: $\theta(z)$ (angle between the molecular director and the layer normal) and $\phi(z)$ (angle between the layer normal and the rubbing direction).

(a) There is a restoring torque against any deviation of the molecules from their equilibrium orientation in the smectic layers.

(b) Twist distortions are forbidden for a perfect smectic; this prohibition can however be relaxed near the transition due to the increase in the layer compressibility and the appearance of a certain density of edge dislocations. Here, we will consider this possibility of twist and will model it with an effective twist elastic constant K_s, which normally is large, but decreases to zero at the transition point.

Condition (b) means that in the SmA phase the molecular reorientation must take place through rotations that change the angle θ between the director and the normal to the smectic layers, any variations of the angle ϕ between the layer normal and the rubbing direction being practically disallowed. However, near the transition K_s must fall and vanish in the N* phase. Consequently, for continuity reasons, there must exist a temperature range in which both θ and ϕ variations are allowed. In this case the total molecular tilt is $\theta+\phi$. A typical profile of the layer orientation in the temperature region of interest is sketched in figure 9. In the N* limit the smectic layers disappear and only the angle $\theta+\phi$ has a physical meaning.

At this point two clarifying remarks should be made. First, we will only consider strong surface anchoring; this means that the layer normal at the surfaces cannot deviate from the rubbing direction. Second, if the anchoring is strong, it should be noted that, strictly speaking, it is the molecules at the surface and not the layer normals which always remain parallel to the rubbing axis. This effect is due to the so-called surface EE [10, 11], which can produce a chiral molecular twist and/or a layer rotation within a very small interfacial region. However, this is a static distortion and cannot be observed in our experiment. Therefore, we have not considered the possible existence of an angle between the rubbing direction and the bulk crystal axis for $E=0$.

We now turn to develop our model more quantitatively. The free energy variation produced by the electric field can be expressed as:

$$\Delta F = \int\left\{\frac{1}{2}a\theta^2 - \mu\theta E + \frac{1}{2}K_2\left[\frac{\partial(\theta+\phi)}{\partial z}\right]^2 + \frac{1}{2}K_s\left[\frac{\partial\phi}{\partial z}\right]^2\right\}dV \qquad (8)$$

where z is the coordinate along the sample thickness and dV the volume element. Apart from the usual contributions, two twist elastic terms have been included. The first is nematic-like and is driven by K_2; the second describes the twist of the layers mentioned above and is null in the N* phase. From equation (8) the following equilibrium equations for θ and ϕ are obtained:

$$K_2\left[\frac{\partial^2\theta}{\partial z^2}+\frac{\partial^2\phi}{\partial z^2}\right] - a\theta + \mu E = 0 \qquad (9)$$

$$K_s\frac{\partial^2\phi}{\partial z^2} + K_2\frac{\partial^2(\theta+\phi)}{\partial z^2} = 0. \qquad (10)$$

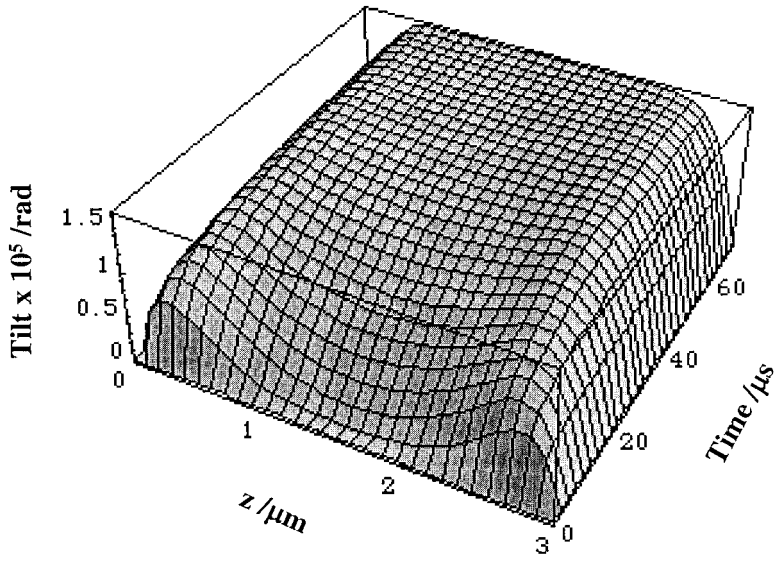

Figure 10. Time dependence of the layer orientations ϕ after the usual electroclinic process according to equation (12). The values assumed for the different parameters are indicated in the text.

Equation (9) is the usual expression for the EE with an additional term accounting for the twist torque due to the inhomogeneity of the molecular orientation near the surfaces. Normally this contribution is negligible. Equation (10), on the other hand, is the torque balance between nematic and smectic twists.

Now we analyse the dynamics of the EE effect when a constant electric field is suddenly applied to the sample at time $t = 0$. The effect of the surfaces is modelled by a z dependent electroclinic coefficient μ. Near the surface at $z = 0$ we will assume

$$\mu = \mu_0 + \mu_1 \exp(-z/\xi) \tag{11}$$

and an analogous expression for the surface at $z = d$. Here ξ is a parameter that defines an effective surface thickness. According to equation (11) μ has an almost constant value in the bulk (μ_0) and increases rapidly near the cell surfaces to a value ($\mu_0 + \mu_1$). On the other hand, a simplification is introduced by considering that the evolution of $\theta(z, t)$ is fast enough to reach its saturation value before $\phi(z, t)$ departs from zero. This approximation decouples the dynamics of θ and ϕ. On the one hand, $\theta(z, t)$ has essentially a Debye dependence with a saturation value $\theta_s(z) \approx E\mu(z)/a$ and a relaxation time $\tau_1 \approx \gamma/a$, where γ is the rotational viscosity; this is the usual fast mechanism. On the other hand, $\phi(z, t)$ follows a simple dynamical equation obtained from equation (10) with the addition of a viscous term:

$$[K_2 + K_s]\frac{\partial^2 \phi}{\partial z^2} + f(z) = \gamma \frac{\partial \phi}{\partial t} \tag{12}$$

where $f(z) = K_2 \partial^2 \theta_s(z)/\partial z^2$. Equation (12) predicts a characteristic time for the ϕ reorientation of the order of

$$\tau_2 = \frac{\gamma d^2}{\pi^2 (K_s + K_2)}. \tag{13}$$

Figure 10 shows a typical solution of equation (12). The following parameters were used: $\gamma = 0.1$ P, $K_2 = 10^{-6}$ dyn, $K_s = 50 \times K_2$, $d = 3\,\mu$m, $\xi = 0.1\,\mu$m, $E\mu_0/\alpha = 3 \times 10^{-5}$ rad, $E\mu_1/\alpha = 1.5 \times 10^{-3}$ rad and $\gamma/\alpha = 1\,\mu$s. The initial condition was $\phi(z, 0) = 0$, and as boundary conditions we set $\phi(0, t) = \phi(d, t) = 0$ (the normal to the smectic layers remains parallel to the rubbing direction at the cell surfaces). Figure 11 shows the evolution of the resultant

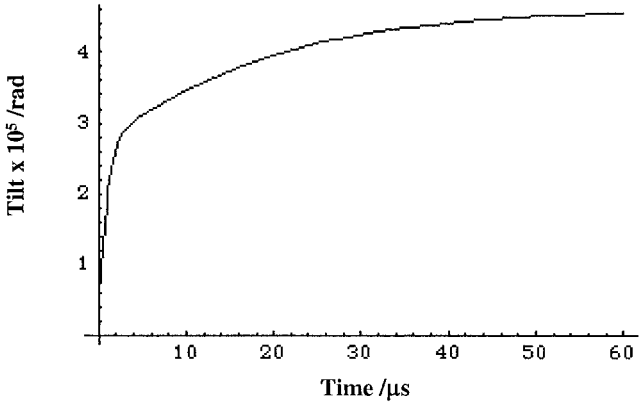

Figure 11. Time dependence of the total molecular tilt angle $\theta + \phi$ at the middle of the cell showing the two-step electroclinic process.

molecular angle at the middle of the cell $\theta(d/2, t)+\phi(d/2, t)$. The two step process is evident. The slow time is about 20 μs in agreement with equation (13), and the proportion of the slow mechanism x is close to unity. As can be seen, these values have the same order of magnitude as those obtained experimentally at the anomalous region.

Finally we make some comments with reference to the N* phase. According to our model, for long enough times, the tilt at the surfaces must propagate without attenuation into the entire sample thickness. Therefore, a rather large EE should result in this phase. We have tried to investigate the nematic EE at low frequencies. However, unfortunately, too low frequencies are necessary to observe this surface-mediated phenomenon. The characteristic time according to equation (13) is $\tau_2 = \gamma d^2/\pi^2 K_2$, which is of the order of 1 ms for $\gamma = 0.1$ P, $K_2 = 10^{-6}$ dyn, and $d = 3$ μm. Figure 12 shows the tan δ results at $T = 92$°C in the low frequency range. Clearly, a departure from linear behaviour takes place below 1 kHz. We have checked however that the data below 1 kHz have unusual features and no clear meaning. For example, tan $\delta > 0$ at the lower limit has, in principle, no physical meaning. In addition, we found that the tan δ values depend on the magnitude of the applied field, and the dependence is stronger as the frequency is lowered. Our hypothesis is that in this frequency range the magnitude of the field is large enough to provoke electrohydrodynamic instabilities in the material, so preventing the possibility of any reliable measurement.

Still, a remarkable characteristic can be noticed in figure 12. If we extrapolate the normal linear behaviour above 1 kHz to low frequencies, the resulting intercept at the origin is unequivocally different from zero.

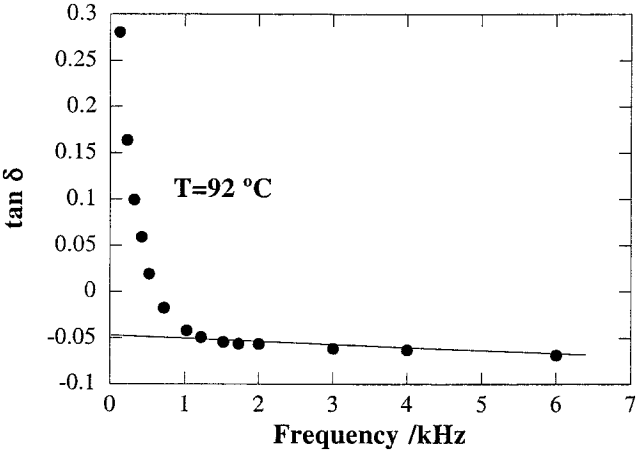

Figure 12. Frequency dependence of tan δ for the N* phase in the low frequency range. A departure from the linear behaviour occurs for $v < 1$ kHz, and the intercept of the straight line at the origin is non-null.

This is what one would expect if a second electroclinic mechanism operated at frequencies $v < 1$ kHz, and so provides indirect evidence of the existence of such a phenomenon. In this respect it is interesting to point out that an analogous effect in which the bend elastic constant K_3 is responsible for the tilt propagation into the bulk was reported in [12] for a homeotropically aligned N* material.

Regarding the effect at high frequencies, it is not evident whether the measured signal comes from the tilt at the surfaces or there is also a tilt inside the material. What is clear is that the response is very small and decreases progressively upon heating, attaining really insignificant values well inside the N* phase. Therefore, the EE is probably due to residual smectic fluctuations (cybotactic groups) with fast relaxation times. We conclude then that no inherent nematic EE exists in the bulk (at least in this material), and the observed phenomenon is just a pretransitional effect which extends over a broad temperature range above the SmA phase.

5. Conclusions

The dynamics of the EE have been studied in a material with SmA and N* phases. Two additive mechanisms with different relaxation times have been identified near the transition. The second process can be explained in terms of a surface-mediated effect driven by elastic forces. Usually, this second mechanism is very small and too fast to be detected in the SmA phase, given the rigidity of the smectic layers. However, it becomes visible near the N* phase, where the layers have almost disappeared and their twist elastic constant decreases rapidly. The first mechanism is the only bulk process inherent to the material and behaves normally at the phase transition. In the N* phase only residual effects due to smectic fluctuations are detected. Therefore, although the intrinsic nematic EE is certainly not forbidden by symmetry [1, 3], it seems that, in practice, translational order is indispensable for the appearance of the phenomenon.

This work was supported by the CICYT of Spain (Project No. MAT2000-1293-C02-02).

References

[1] Li, Z., Petschek, R. G., and Rosenblatt, C., 1989, *Phys. Rev. Lett.*, **62,** 796.
[2] Li, Z., Di Lisi, G. A., Petschek, R. G., and Rosenblatt, C., 1990, *Phys. Rev. A*, **41,** 1997.
[3] Etxebarria, J., and Zubia, J., 1991, *Phys. Rev. A*, **44,** 6626.
[4] Li, Z., Akins, R. B., Di Lisi, G. A., Rosenblatt, C., and Petschek, R. G., 1991, *Phys. Rev. A*, **43,** 852.
[5] Li, Z., Ambigapathy, R., Petschek, R. G., and Rosenblatt, C., 1991, *Phys. Rev. A*, **43,** 7109.

[6] Zubia, J., Etxebarria, J., and Pèrez-Jubindo, M. A., 1994, *Liq. Cryst*., **16,** 941.
[7] Nounesis, G., Garland, C. W., and Shashidhar, R., 1991, *Phys. Rev. A*, **43,** 1849.
[8] Blinc, R., and Zeks, B., 1978, *Phys. Rev. A*, **18,** 740.
[9] Xu, J., Selinger, R. L. B., Selinger, J. V., Ratna, B. R., and Shashidhar, R., 1999, *Phys. Rev. E*, **60,** 5584.
[10] Xue, J., and Clark, N. A., 1990, *Phys. Rev. Lett*., **64,** 307.
[11] Spector, M. S., Prasad, S. K., Weslowski, B. T., Kamien, R. D., Selinger, J. V., Ratna, B. R., and Shashidhar, R., 2000, *Phys. Rev. E*, **61,** 3977.
[12] Crandall, K. A., Tripathi, S., and Rosenblatt, C., 1992, *Phys. Rev. A*, **46,** R715.